Article

Cell Chemical Biology

A Small Molecule Targeting the Transmembrane Domain of Death Receptor p75^{NTR} Induces Melanoma Cell Death and Reduces Tumor Growth

Graphical Abstract

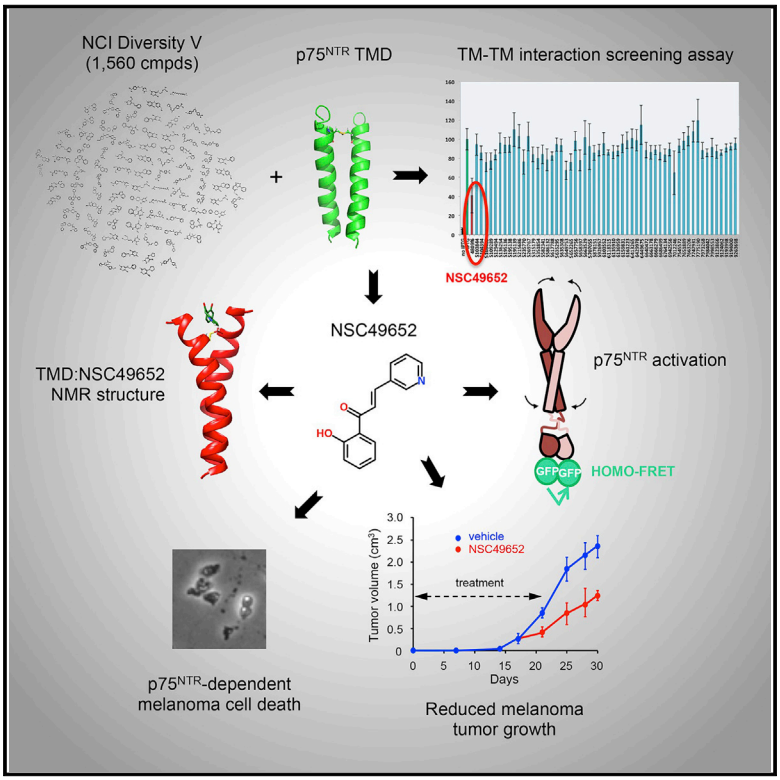

Authors

Eddy T.H. Goh, Zhi Lin, Bo Young Ahn, ..., Brian Dymock, Donna L. Senger, Carlos F. Ibáñez

Correspondence

phscfi@nus.edu.sg

In Brief

Small molecules offer powerful ways to alter protein function. However, most proteins in the human proteome lack small-molecule probes. Goh et al. Identified a small molecule that interacts with the transmembrane domain of death receptor p75^{NTR}, which induces melanoma cell death, and inhibits melanoma tumor growth *in vivo*.

Highlights

- We identified a compound targeting the transmembrane domain of death receptor p75^{NTR}
- NSC49652 induced profound conformational changes and receptor activity
- NSC49652 induced melanoma cell death, and inhibited melanoma tumor growth *in vivo*
- TMDs represent attractive targets for small-molecule manipulation of receptor function

Goh et al., 2018, Cell Chemical Biology *25*, 1485–1494
December 20, 2018
https://doi.org/10.1016/j.chembiol.2018.09.007

CellPress

Cell Chemical Biology
Article

A Small Molecule Targeting the Transmembrane Domain of Death Receptor p75^{NTR} Induces Melanoma Cell Death and Reduces Tumor Growth

Eddy T.H. Goh,[1,2,3,9] Zhi Lin,[1,2,7,9] Bo Young Ahn,[4,9] Vanessa Lopes-Rodrigues,[1,2] Ngoc Ha Dang,[4] Shuhailah Salim,[1,2] Bryan Berger,[5] Brian Dymock,[6,8] Donna L. Senger,[4] and Carlos F. Ibáñez[1,2,3,10,*]
[1]Department of Physiology, National University of Singapore, Singapore 117597, Singapore
[2]Life Sciences Institute, National University of Singapore, Singapore 117456, Singapore
[3]Department of Cell and Molecular Biology, Karolinska Institute, Stockholm 17165, Sweden
[4]Arnie Charbonneau Cancer Institute, Department of Oncology, Cumming School of Medicine, University of Calgary, Calgary T2N 1N4, Canada
[5]Department of Chemical Engineering, University of Virginia, Charlottesville, VA 22904, USA
[6]Department of Pharmacy, National University of Singapore, Singapore 117597, Singapore
[7]Present address: School of Life Sciences, Tianjin University, Tianjin, China
[8]Present address: Monash University, Melbourne, Australia
[9]These authors contributed equally
[10]Lead Contact
*Correspondence: phscfi@nus.edu.sg
https://doi.org/10.1016/j.chembiol.2018.09.007

SUMMARY

Small molecules offer powerful ways to alter protein function. However, most proteins in the human proteome lack small-molecule probes, including the large class of non-catalytic transmembrane receptors, such as death receptors. We hypothesized that small molecules targeting the interfaces between transmembrane domains (TMDs) in receptor complexes may induce conformational changes that alter receptor function. Applying this concept in a screening assay, we identified a compound targeting the TMD of death receptor p75^{NTR} that induced profound conformational changes and receptor activity. The compound triggered apoptotic cell death dependent on p75^{NTR} and JNK activity in neurons and melanoma cells, and inhibited tumor growth in a melanoma mouse model. Due to their small size and crucial role in receptor activation, TMDs represent attractive targets for small-molecule manipulation of receptor function.

INTRODUCTION

Transmembrane receptors mediate transfer of information across the plasma membrane. A crucial element in this process is the transmembrane domain (TMD), a stretch of approximately 20 amino acids linking extracellular and intracellular receptor domains. Several studies have shown that conformational changes induced by ligand binding to extracellular domains cause relative movements of TMDs in dimeric or oligomeric receptor complexes which in turn trigger conformational changes in intracellular domains leading to intracellular signaling (Arkhipov et al., 2013; Endres et al., 2013; Grigoryan et al., 2011). TMDs are therefore critical structural elements for information transfer across the plasma membrane. The question then arises whether TMDs are suitable targets for small molecules to affect receptor function. TMDs are small and often quite divergent, even within families of related receptors. Small molecules targeting molecular interfaces between TMDs in receptor complexes may induce or perturb conformational changes in TMDs and hence constitute useful chemical probes for acute and reversible modulation of receptor activity.

Death receptors are characterized by the presence of a globular domain in their intracellular region known as the "death domain" (Ferrao and Wu, 2012; Park et al., 2007). Prototypical death receptors include tumor necrosis factor receptor 1 (TNFR1), the Fas receptor (CD95), and the p75 neurotrophin receptor (p75^{NTR}, also known as NGFR, TNFRSF16, and CD271). p75^{NTR} signaling can induce apoptotic cell death in subpopulations of neurons and cancer cells, and has therefore emerged as an interesting target for manipulation by small molecules. Neurotrophins engage p75^{NTR} through large molecular interfaces. Moreover, lacking enzymatic activity, death receptors signal by forming complexes with intracellular effectors that also involve relatively large molecular surfaces. It is therefore difficult for small molecules to affect the protein-protein interactions that lead to the activation of these receptors. Many death receptors reside at the plasma membrane as pre-formed dimers or trimers stabilized by either covalent or non-covalent interactions between different receptor domains, including the TMDs. A highly conserved Cys residue in the p75^{NTR} TMD (Cys^{256}, human p75^{NTR} numbering) forms a disulfide bridge that covalently links two receptor protomers (Vilar et al., 2009). In the absence of this TM Cys, p75^{NTR} still form dimers through non-covalent interactions mediated by other TMD residues (Vilar et al., 2009) as well as the death domain (Lin et al., 2015). On the other hand, the TMD Cys is critical for ligand-mediated receptor activation by allowing a scissor-like movement of TMDs that results in

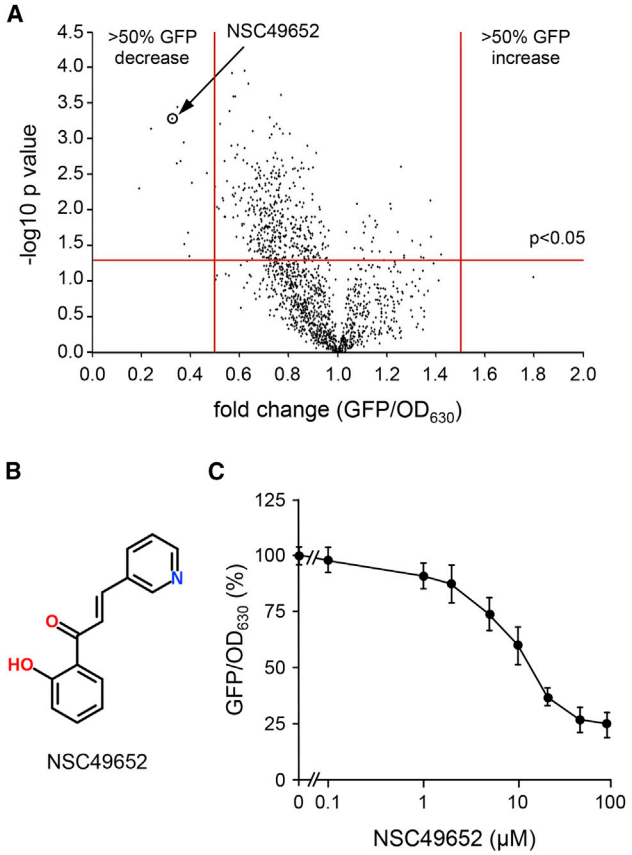

Figure 1. Small-Molecule NSC49652 Affects the Interaction of p75^{NTR} TMDs

(A) Volcano plot of AraTM screening assay on NCI Diversity V compound library. A total of 1,580 compounds dispensed in twenty 96-well plates were screened at 50 μM in three independent runs. Fold change was calculated against the corresponding vehicle (DMSO) control of each plate. Hits were defined as compounds resulting in greater than ±0.5-fold change in GFP/optical density at 630 nm (OD_{630}) signal without affecting OD_{630} by greater than 0.3-fold across the three runs. Compound NSC49652 is indicated.

(B) Chemical structure of NSC49652.

(C) Dose response of NSC49652 in the AraTM assay of p75^{NTR} TMDs. Results are plotted as means ± SD (N = 3). The half maximal inhibitory concentration (10 μM) was calculated as the dose that resulted in half maximal response.

the transient separation of death domains and recruitment of intracellular effectors (Lin et al., 2015; Vilar et al., 2009). Mutant p75^{NTR} molecules lacking the TM Cys residue are unable to respond to neurotrophin ligands despite showing normal cell surface expression and ligand binding (Tanaka et al., 2016; Vilar et al., 2009).

The crucial role played by the p75^{NTR} TMDs in the mechanism of receptor activation prompted us to investigate whether small molecules targeting this TMD can affect receptor function. Such molecules may function by altering TMD oligomerization or relative conformation at the plasma membrane. In this study, we used a method to screen and identify small molecules targeting the interfaces between TMD complexes in transmembrane receptors. We characterized one compound that interacts with the p75^{NTR} TMD, induces conformational changes and activity in the full-length receptor in mammalian cells, and inhibits melanoma tumor growth in mice in a p75^{NTR}-dependent manner.

RESULTS

Identification of a Small Molecule Targeting the p75^{NTR} TMD

We adapted the AraTM transcription factor-based system in bacteria (Russ and Engelman, 1999; Su and Berger, 2013) to develop a screening assay to identify small molecules capable of affecting the strength of interaction or relative conformation of p75^{NTR} TMDs in a biological membrane (see the STAR Methods section for details). To facilitate access of small molecules across the bacterial cell wall, we used *E. coli* strain AS19 lacking lipopolysacharide, which previous studies have shown to allow the entry of large macromolecules (Good et al., 2000). We screened a prototype library of 1,580 chemically diverse compounds from the National Cancer Institute and identified several molecules that affected TMD-TMD interactions as determined by a statistically significant decrease in the GFP readout normalized to bacterial density (Figure 1A). After further validation experiments and controls for unspecific effects on bacteria viability, five compounds were identified that reproducibly affected TMD interactions in this assay (Figures 1B and S1A). The two most potent of these, NSC149286 and NSC49652, shared similar structural characteristics; and the more active of the two, NSC49652 (CAS no. 908563-68-8), was selected for further study. NSC49652 is a chalcone flavonoid consisting of two aromatic rings joined by a three-carbon α,β-unsaturated carbonyl system with a molecular weight of 225.24 Da (Figure 1B). In dose-response studies, NSC49652 displayed a half maximal inhibitory concentration (IC50) of 10 μM in the AraTM assay (Figure 1C). We further tested a manually curated collection of 68 compounds with structures related to that of NSC49652 (Figure S1B). Seven compounds were found to display some level of activity, but none was as potent as NSC49652 at reducing GFP signal in the assay (Figure S1C). Together, these structure-activity studies suggested that the chalcone system (ArCOC = CAr) with ortho-hydroxyl appears to be important for activity, while the 3-pyridyl does not appear to retain activity outside the 2-hydroxy-chalcone core structure. As the α,β-unsaturated carbonyl group may be prone to reactivity with Cys thiol groups, and the TMD of p75^{NTR} contains a Cys residue, we tested whether the inhibitory effect of NSC49652 in the AraTM assay could be reversed after compound wash-out. Following a 4-hr isopropyl β-D-1-thiogalactopyranoside (IPTG) induction in the absence or presence (10–30 μM) of NSC49652, bacterial cells were switched to medium without either IPTG or compound for an additional 2 or 5 hr, and the response compared with that without wash-out (0 hr). At all concentrations tested, removal of compound showed significant recovery of the GFP/optical density at 630 nm signal (Figure S2A), suggesting that the effect of NSC49652 was reversible. In agreement with this, replacement of Cys with Ser in the p75^{NTR} TMD did not affect the activity of NSC49652 in the AraTM assay (Figure S2B), indicating that its effect was not mediated by covalent reaction with the Cys residue.

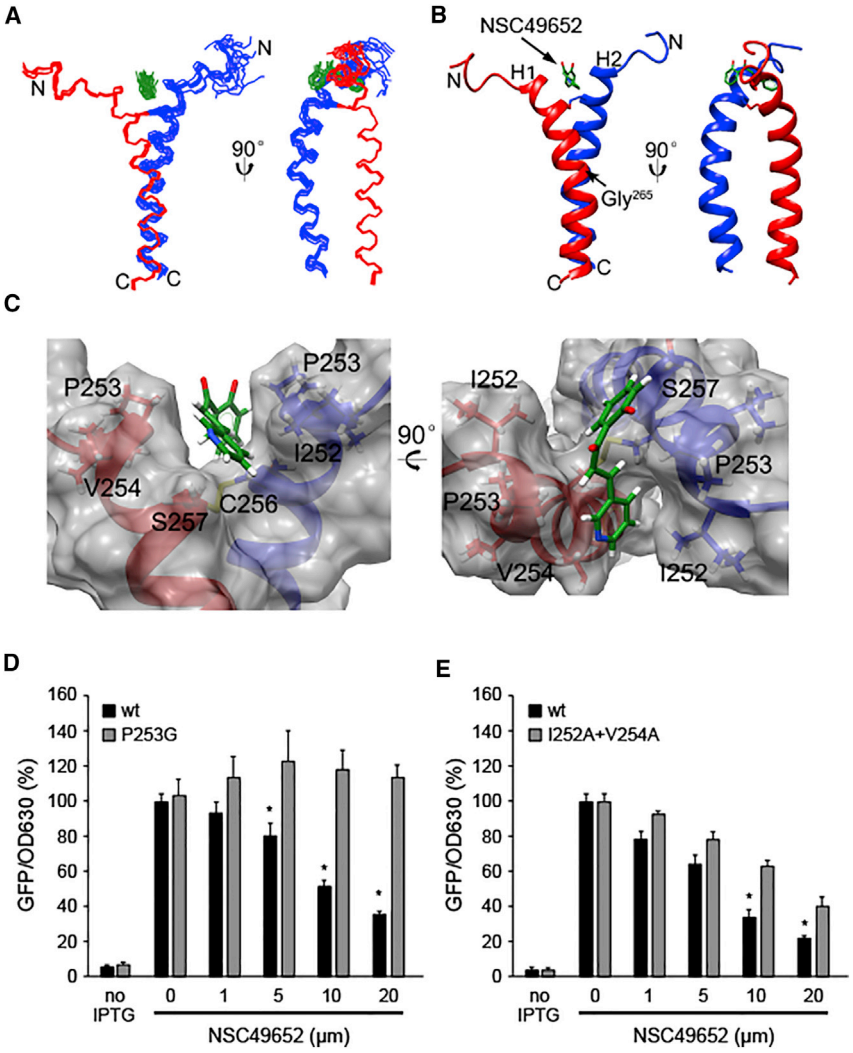

Figure 2. Solution Structure of the Complex between p75^{NTR} TMD and NSC49652 and Structure-Function Analysis of TMD Residues Engaged by NSC49652

(A) Superposition of backbone heavy atoms of the ten lowest-energy structures of the human p75^{NTR} TMD dimer in complex with NSC49652. Monomers of p75^{NTR} TMD dimer are colored in red and blue; NSC49652 is colored in green.

(B) Ribbon drawing of the lowest-energy conformer. NSC49652 (green) and Cys^{256}-Cys^{256} disulfide linkage are shown in stick models.

(C) Binding interface in the complex between the p75^{NTR} TMD dimer and NSC49652 shown as a surface model. Key residues at the binding interface are labeled and depicted as stick models.

(D) Comparison of wild-type p75^{NTR} TMD and P253G mutant in the AraTM assay in response to increasing doses of NSC49652. "No IPTG" denotes the baseline level in the absence of IPTG induction. The GFP over OD_{630} signal without any drug added was set at 100%. Results are plotted as means ± SD (N = 3). *p < 0.05.

(E) Comparison between wild-type p75^{NTR} TMD and I252A/V254A double mutant in the AraTM assay in response to increasing doses of NSC49652. Results are plotted as means ± SD (N = 3). *p < 0.05.

disulfide bond (human p75^{NTR} numbering) and a number of hydrophobic interactions involving Leu, Val, Ile, Ala, Pro, and Trp residues. The TMDs in the complex formed an asymmetrical dimer with a buried area of ~370 Å. NSC49652 bound to a pocket formed by Ile^{252}, Pro^{253}, Val^{254}, Cys^{256}, and Ser^{257} residues in each of the two TMD protomers (Figure 2C). Mutation of Pro^{253} abolished the ability of NSC49652 to affect the p75^{NTR} TMD (Figure 2D), suggesting that it is a key residue for drug binding. Double mutation of Val^{254} and Ile^{252}, but not the individual mutations, also reduced the effect of NSC49652 in the AraTM assay (Figure 2E). None of these mutations diminished baseline interaction between TMDs in the absence of drug (Figures S2C and S2D), suggesting that NSC49652 interacted with p75^{NTR} TMD residues that do not normally contribute to TMD dimerization. The fact that point mutations abolished or diminished the effects of NSC49652 in the AraTM assay suggests that the compound targeted the TM domain and not the technology of the assay. In agreement with this, NSC49652 had no effect on the interaction between the TMDs of α2β3 integrin (Figure S2E).

Solution NMR Structure of NSC49652 in Complex with the p75^{NTR} TMD

Evidence indicating a direct interaction between NSC49652 and the TMD of p75^{NTR} was obtained from chemical shift perturbations and inter-molecular Nuclear Overhauser Effect (NOE) signals derived from 2D and 3D nuclear magnetic resonance (NMR) experiments, respectively, using purified recombinant p75^{NTR} TMD (Figure S3A) in the absence or presence of NSC49652 at a 4.8 molar excess (Figures S3B–S3D). Previous titration experiments had indicated that saturation of binding was achieved between 4 and 5 molar excess of compound. Addition of an inactive compound at the same ratio and concentration did not produce any chemical shift changes in the 2D HSQC spectrum of the p75^{NTR} TMD (Figure S3E). The solution structure of the p75^{NTR} TMD:NSC49652 complex was determined by multidimensional NMR (Figures 2A–2C and S2F) under conditions that were identical to those previously used to determine the structure of p75^{NTR} TMD in the absence of any ligand (Nadezhdin et al., 2016). NSC49652 binds at the N terminus of the p75^{NTR} TMD. The p75^{NTR} TMD:NSC49652 complex adopted a compact quaternary structure restrained by the Cys^{256}-Cys^{256}

NSC49652 Alters the Relative Conformation of p75^{NTR} TMDs and Induces Dynamic Changes in the Full-Length Receptor in Mammalian Cells

Comparison of the structures of the p75^{NTR} TMD dimer in complex with NSC49652 and in its absence (Nadezhdin et al., 2016) revealed significant conformational rearrangement of TMD helices upon NSC49652 binding (Figure 3A). The two helices in the TMD:NSC49652 complex showed kink angles of about

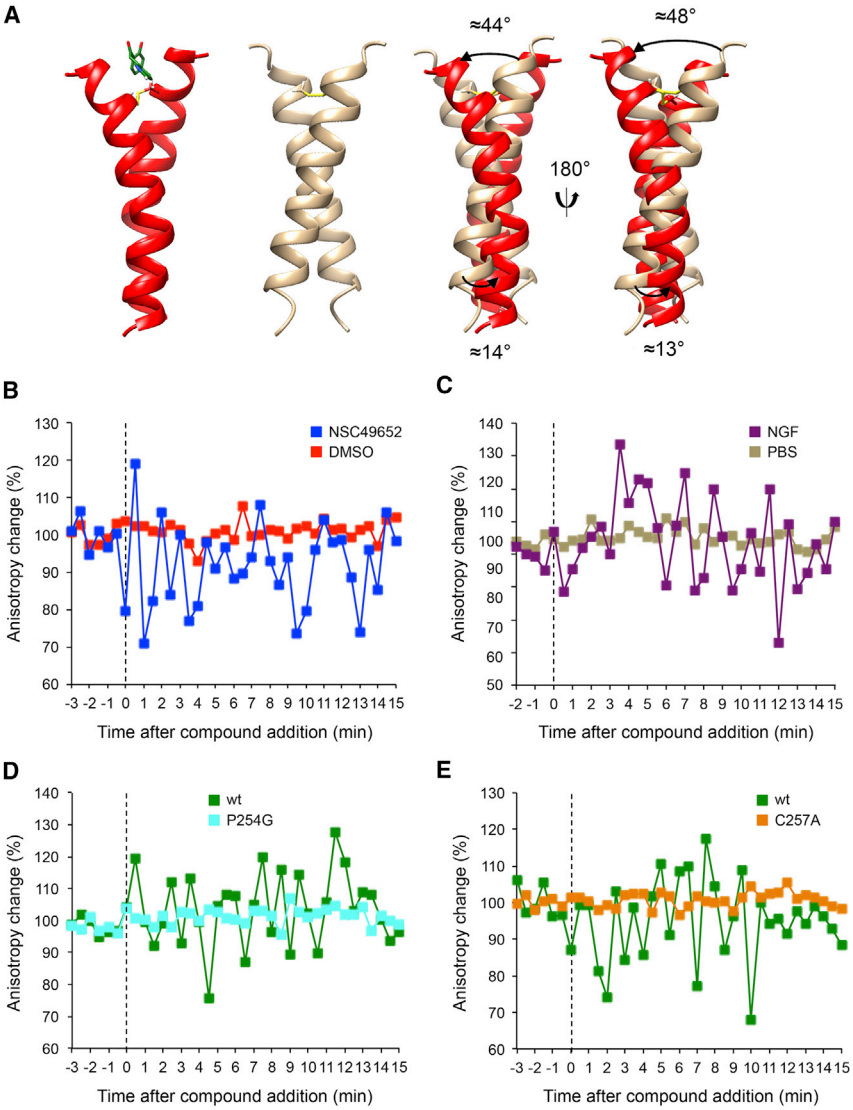

Figure 3. NSC49652 Alters the Relative Conformation of p75^{NTR} TMDs and Induces Dynamic Changes in the Full-Length Receptor in Mammalian Cells

(A) Structural comparison of p75^{NTR} TMD dimers in the presence (red) and absence (brown) of NSC49652 (green). The disulfide bond is indicated in yellow. The model without drug was derived from PDB: 2MIC (Nadezhdin et al., 2016), produced under the same conditions used in the present study. The two models are shown alone (left) and superimposed to each other (right) to highlight their differences. Angle changes induced in the complex with NSC49652 are indicated.

(B) Live cell homo-FRET anisotropy of p75^{NTR} in COS cells in response to NSC49652. Shown are representative traces of average anisotropy change after addition of NSC49652 (20 μM at 0 min) or vehicle in cells expressing wild-type human p75^{NTR}.

(C) Live cell homo-FRET anisotropy of full-length rat p75^{NTR} in COS cells in response to NGF. Shown are representative traces of average anisotropy change after addition of NGF (50 ng/mL at 0 min) or vehicle (PBS) in cells expressing wild-type human p75^{NTR}.

(D) Live cell homo-FRET anisotropy of wild-type and P254G mutant (rat numbering, equivalent to human Pro^{253}) p75^{NTR} in COS cells in response to NSC49652. Shown are representative traces of average anisotropy change after addition of NSC49652 (at 0 min).

(E) Live cell homo-FRET anisotropy of wild-type and C257A mutant (rat numbering, equivalent to human Cys^{256}) p75^{NTR} in COS cells in response to NSC49652. Shown are representative traces of average anisotropy change after addition of NSC49652 (at 0 min).

30° and 35°, respectively, centered on Gly^{265}. In the N terminus upstream of Gly^{265}, the helical segments appeared rotated by 44° and 48°, respectively, compared with the TMD dimer in the absence of compound (Figure 3A), creating a hydrophobic pocket for drug binding. The C-terminal segments displayed smaller shift angles of 13° and 14°, respectively, perhaps restricted by bulky side chain residues in that area (i.e., Leu^{266}, Ile^{270}, and Arg^{274}). To determine whether the conformational changes induced by NSC49652 on the p75^{NTR} TMDs as detected by NMR have any relevance for the function of the receptor on the plasma membrane of mammalian cells, we conducted real-time homo-FRET anisotropy experiments (Figure S2F). Previous studies by us and others have shown that the intracellular death domains of p75^{NTR} are associated with each other (high FRET, low anisotropy state) under basal conditions (Lin et al., 2015; Sykes et al., 2012; Vilar et al., 2009), but ligand engagement induces transient separation of p75^{NTR} death domains (low FRET, high anisotropy state) manifested as large oscillations in real-time anisotropy measurements (Vilar et al., 2009). These changes are abolished in mutant p75^{NTR} molecules lacking the conserved transmembrane Cys residue (Cys^{256} in human, Cys^{257} in rat p75^{NTR}), despite normal ligand binding (Lin et al., 2015; Tanaka et al., 2016; Vilar et al., 2009). (We note that the TMDs of human and rat p75^{NTR} are identical in sequence.) COS cells expressing full-length, GFP-tagged rat p75^{NTR} were treated with vehicle or NSC49652 and changes in anisotropy levels were recorded over time. NSC49652 induced large oscillations in real-time anisotropy (Figure 3B), similar to those induced by endogenous p75^{NTR} ligands, such as nerve growth factor (NGF) (Figure 3C). In agreement with the AraTM and NMR binding data, mutation of transmembrane Pro^{254} (equivalent to human Pro^{253}) to Gly also blunted homo-FRET changes induced by NSC49652 (Figure 3D). Interestingly, as in the case of p75^{NTR} activation by NGF (Tanaka et al., 2016; Vilar et al., 2009), mutation of transmembrane Cys^{257} (rat p75^{NTR} numbering) completely abolished death domain movements in response to NSC49652 (Figure 3E). Together, these findings suggest that NSC49652 binding to the TMD of p75^{NTR} induces conformational changes that can be propagated to intracellular death domains, resembling receptor activation by endogenous p75^{NTR} ligands.

NSC49652 Induces Apoptosis through p75^{NTR} and the JNK Pathway in Neurons and Affects the Viability of Melanoma Cells

Activation of p75^{NTR} induces apoptotic cell death in different types of cells, including neurons and some cancer cells (Ichim et al., 2012; Underwood and Coulson, 2008). We tested whether NSC49652 affected the ability of p75^{NTR} to induce apoptotic cell death in response to NGF in primary cultures of mouse cerebellar granule neurons by assessing the levels of activated (cleaved) isoforms of caspase-3 and poly(ADP) ribose polymerase (PARP), two commonly used markers of apoptosis. We found that NSC49652 could induce an apoptotic response on its own in these neurons independently of NGF (Figure 4A), suggesting that it behaves as a functional p75^{NTR} agonist in this regard. The effect of NSC49652 on caspase-3 activation could be suppressed by a specific inhibitor of JNK (c-Jun N-terminal kinase) (Figure 4B), a known mediator of apoptosis induced by p75^{NTR}. Next, we tested the responses of neurons derived from p75^{NTR} knockout mice, which lack the receptor entirely, or from two strains of knockin mice, one lacking only the p75^{NTR} death domain (ΔDD), the other carrying a mutation in the TM Cys residue (C259A, mouse p75^{NTR} numbering), both of which are crucial for receptor activity (Tanaka et al., 2016). We found that, while NSC49652 induced apoptosis in wild-type cells, all mutant neurons showed resistance at the tested concentrations (Figures 4C–4E). Together, these data suggested that NSC49652 can induce neuronal cell death through p75^{NTR} and the JNK pathway in neurons. As several cancer cells, particularly neural crest-derived melanoma, express high levels of p75^{NTR}, we tested whether NSC49652 could induce apoptosis in three different lines of human melanoma, namely A875, 70W, and 3S5. NSC49652 induced activation of PARP in all three cell lines (Figures 4F and 4G). shRNA knockdown of p75^{NTR} in A875-GFPLuc melanoma cells (a derivative of A875, see the STAR Methods and Figure S4A) significantly reduced the pro-apoptotic effects of NSC49652 (Figure 4H). An analysis of dose-dependent effects of NSC49652 on cell viability showed a differential sensitivity between control and knockdown cells up to 50 μM (Figure 4I). At 100 μM and above, both cell lines were sensitive to the compound (Figure 4I), indicating *in vitro* off-target effects at the highest concentrations, which is not unusual for chemotherapeutic drugs.

Oral Administration of NSC49652 Reduces Tumor Growth and Improves Survival in a Human Melanoma Xenograft Model

The effects of NSC49652 on melanoma cells prompted us to investigate whether the compound may have similar effects *in vivo*. To determine optimal dosing of NSC49652, initial pharmacokinetic assessment was performed following a single oral (gavage) administration of 10 mg/kg NSC49652. Plasma concentrations of NSC49652 were quantifiable up to 24 hr, with a peak plasma concentration of 2,117.51 ng/mL (C_{max}, 9.4 μM) attained at 0.25 hr (T_{max}), and an oral bioavailability of 29%. Mean pharmacokinetic parameters for NSC49652 are summarized in Figures S5A and S5B. Next, to establish the maximal dosing for the *in vivo* studies, toxicology studies were performed on a 3-week repeated-dose schedule (5 days on; 2 days off) in both male and female C57BL/6 mice. Oral administration of NSC49652 to a maximal concentration of 200 mg/kg was performed with no mortality or adverse clinical signs observed in any of the NSC49652-treated mice. Assessment of clinical signs included body weight, food consumption, plasma chemistry, gross pathology, and histopathologic examination. In addition, as the preclinical studies would be performed using immunodeficient (severe combined immunodeficiency [SCID]) mice, 200 mg/kg NSC49652 was also administered to SCID mice for 1 week with no treatment-related effects observed. Based on these toxicity studies, a treatment schedule of three cycles of 200 mg/kg NSC49652 administered via oral gavage on a 5-day on, 2-day off regime was selected for the *in vivo* efficacy studies. In brief, human melanoma xenografts were established using A875-GFPLuc melanoma cells (carrying a luciferase reporter) implanted subcutaneously on the flank of SCID mice. The luciferase signal allows for early detection of tumor burden. There were no significant differences in the growth rates of control (NT) and p75^{NTR} knockdown (shp75) cells *in vitro* (Figures S4B–S4D). Treatment with NSC49652 was initiated once tumors were detectable by luciferase imaging. Following completion of the 3-week drug regime, animals were monitored daily and sacrificed when the tumors exceeded 2 cm^3 (survival time). We compared tumor growth and survival in mice that received control A875-GFPLuc cells (non-targeting [NT]) or p75^{NTR} knockdown cells (shp75). Loss of p75^{NTR} expression was maintained *in vivo* in the knockdown cells as verified by immunohistochemistry (Figure S4E). Treatment with NSC49652 significantly inhibited the growth of tumors derived from A875-GFPLuc cells compared with vehicle-treated animals in three independent experiments (Figures 5A, S5C, and S5D, respectively). By 30 days, all vehicle-treated animals that received A875-GFPLuc NT cells expressing p75^{NTR} had been sacrificed (Figure 5B), and their median survival time was 28 days. In contrast, the maximal survival time of animals treated with NSC49652 was 48 days (Figure 5B), with a median survival of 36 days. Tumors produced by A875-GFPLuc shp75 knockdown cells, although smaller than those generated by control NT cells, were not affected by NSC49652 treatment (Figures 5A, S8A, and S8B), supporting the notion that NSC49652 functioned by targeting p75^{NTR}. Finally, the tumors of the animals treated with NSC49652 showed a significant increase in TUNEL staining compared with vehicle control-treated animals (Figures 5C and 5D), indicating increased cell death *in vivo* as a result of the treatment.

DISCUSSION

In this study, we describe the identification of a small molecule that interacts with the TMD of death receptor p75^{NTR}, induces conformational changes and activity in the full-length receptor in mammalian cells, and inhibits melanoma tumor growth in mice in a p75^{NTR}-dependent manner. Compound NSC49652 bound to a pocket in the p75^{NTR} TMD dimer that is not present in the known conformation of the unbound dimer, suggesting that either NSC49652 induces a new conformation or stabilizes a pre-existing, but less frequent, configuration of these TMDs. This question could be resolved by further studies of the dynamics of the p75^{NTR} TMDs in biological membranes. The conformation change observed in the NMR structure was mirrored by the effects of NSC49652 on homo-FRET anisotropy

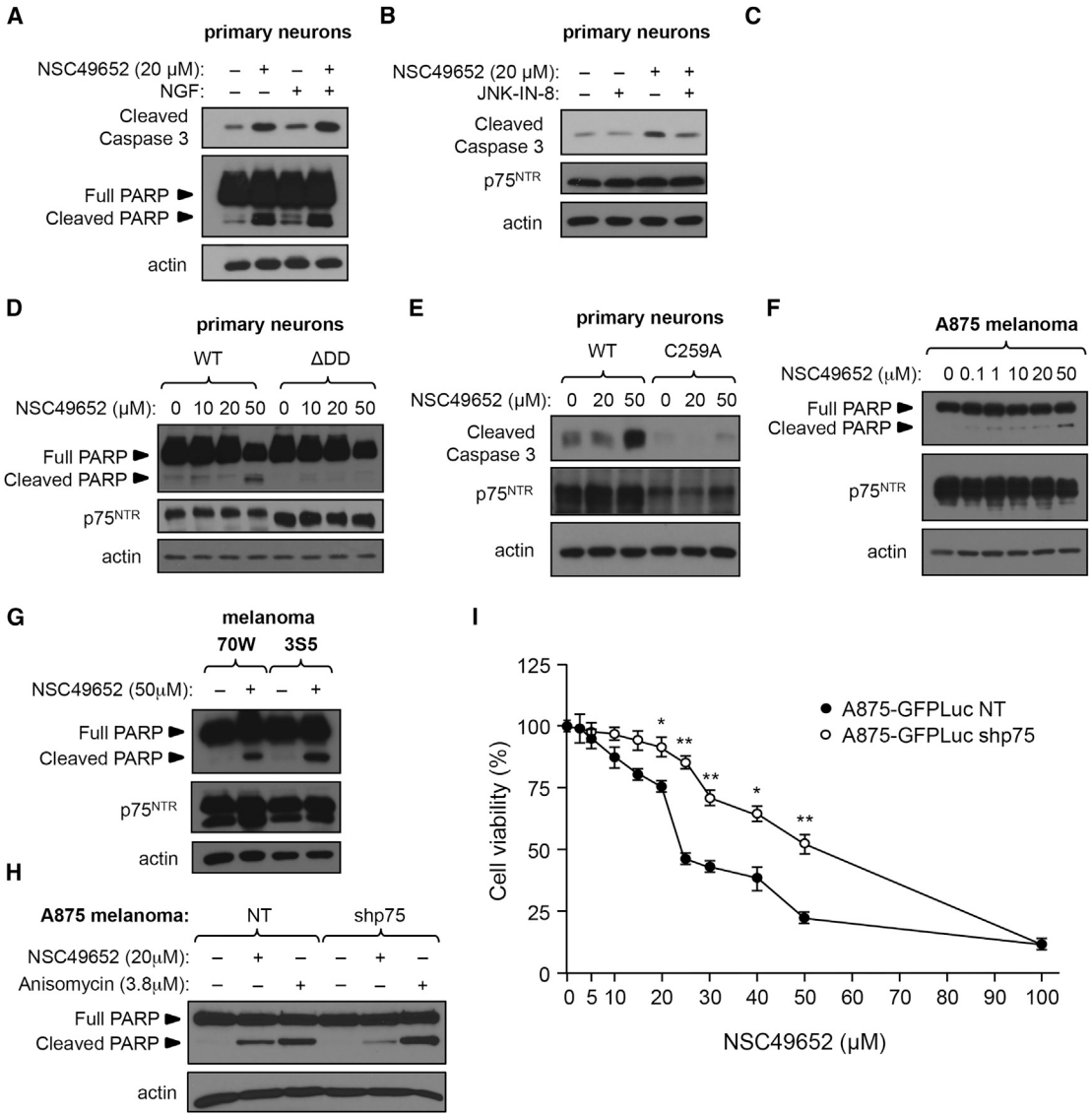

Figure 4. NSC49652 Induces Apoptosis through p75^{NTR} and the JNK Pathway in Neurons and Affects Viability of Melanoma Cells

(A) Representative western blot analysis showing induction of apoptotic markers (cleaved caspase-3 and PARP) by NGF and NSC49652 in cultures of post-natal day 5 (P5) rat cerebellar granule neurons (CGNs) assessed by western blotting. Blots were reprobed with antibodies against actin. The experiment was repeated three times with comparable results.

(B) Representative western blot analysis showing induction of cleaved caspase-3 by NSC49652 in the presence and absence of JNK inhibitor JNK-IN-8 (3 μM) in cultures of P5 rat CGNs assessed by western blotting. Blots were reprobed with antibodies against actin. The experiment was repeated three times with comparable results.

(C–E) Representative western blot analysis showing induction of cleaved caspase-3 (C and E) or PARP (D) by NSC49652 in cultures of P7 mouse CGNs derived from wild-type (WT) mice and p75^{NTR} knockout (C), ΔDD (D), or C259A (E) mutant mice. Blots were reprobed with antibodies against p75^{NTR} extracellular domain and actin. The experiment was repeated three times with comparable results.

(F–G) Representative western blot analysis showing induction of cleaved PARP in human A875 (F), 70W, and 3S5 (G) cell lines in response to 4 hr treatment with the indicated concentrations of NSC49652. The experiment was repeated three times with comparable results. Unlike primary neurons, robust induction of cleaved caspase-3 was difficult to obtain in melanoma cells.

(H) Representative western blot analysis showing induction of cleaved PARP in A875 control (NT [non-targeting]) and knockdown (shp75) cells in response to NSC49652 (20 μM) or anisomycin (3.8 μM). The experiment was repeated three times with comparable results.

(I) Dose-dependent cell viability of A875 control (NT) and knockdown (shp75) cells in response to NSC49652. Results are plotted as means ± SD (N = 3). *$p < 0.05$; **$p < 0.01$.

in the intact receptor in mammalian cells, suggesting they may be related. The oscillations in anisotropy caused by NSC49652 indicate dynamic changes in p75^{NTR} intracellular domains, possibly reflecting rapid opening and closing of death domain dimers, a response that is very similar to that elicited by neurotrophin ligands of p75^{NTR} and which allows the binding of

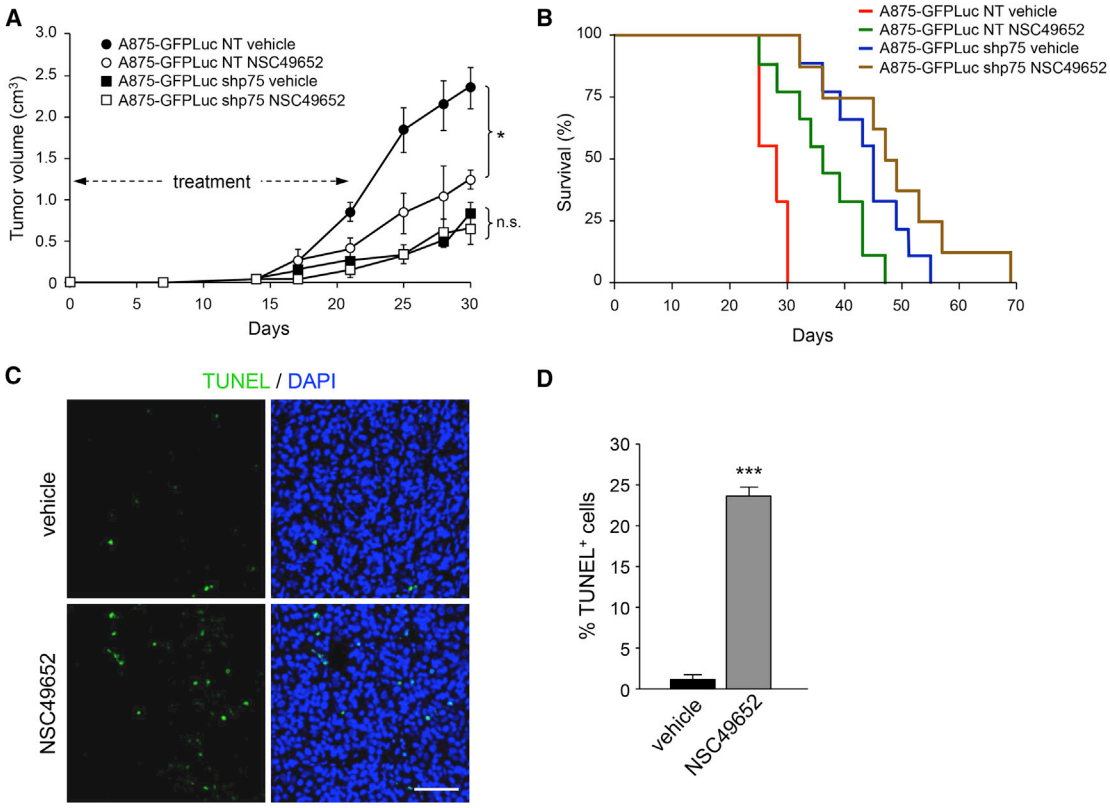

Figure 5. Oral Administration of NSC49652 Reduces Tumor Growth and Improves Survival in a Human Melanoma Xenograft Model

(A) Quantitative assessment of tumor burden as measured every other day using a caliper. NSC49652 was administered orally during the first 3 weeks. Data are presented as means ± SEM (N = 10 mice per group). *p < 0.05; n.s., not significant. A875-GFPLuc NT (non-targeting), control cell line; A875-GFPLuc shp75, $p75^{NTR}$ knockdown cell line.

(B) Kaplan-Meier assessment of survival following treatment with NSC49652 or vehicle as indicated. p < 0.0001 (log rank test) for NSC49652 compared with vehicle in A875-GFPLuc NT.

(C) Representative images of formalin-fixed, paraffin-embedded tumor sections stained by TUNEL from vehicle- or NSC49652-treated animals bearing A875-GFPLuc NT tumors. Total cell nuclei were visualized using DAPI- (blue) and apoptotic TUNEL-positive cells (fluorescein-dUTP) are green. Scale bar, 15 μm.

(D) Apoptotic index in vehicle- or NSC49652-treated A875-GFPLuc NT tumors expressed as the ratio of the number of TUNEL-positive cells to the number of DAPI-positive cells per field of view. Data are expressed as means ± SEM from three independent fields (two mice/group) using a 40× microscopic field. Means that are significantly different from controls are indicated as ***p < 0.001.

intracellular effectors to the receptor (Lin et al., 2015; Tanaka et al., 2016). Interestingly, the anisotropy changes induced by NSC49652 were abolished upon mutation of TMD Cys^{256}, which is also required for neurotrophin-induced receptor activation (Vilar et al., 2009). Together, the results from our NMR and FRET studies explain why NSC49652 displayed agonistic activity on full-length $p75^{NTR}$ despite decreasing the GFP signal in the AraTM assay. Based on these observations, we suggest that binding of NSC49652 to the $p75^{NTR}$ TMD biases the conformation of the receptor in a manner that allows induction of cell death signaling in neurons and melanoma cells. The conformational changes induced by NSC49652 on the $p75^{NTR}$ TMD, as detected by our structure, represent the first structural glimpse into a possible mechanism for transmembrane coupling in this receptor, an advance that would have been difficult to achieve without chemical biology.

Previous attempts to target $p75^{NTR}$ have focused on the receptor extracellular domain, with the idea to either block or mimic its interaction with neurotrophin ligands. Two small molecules reported to target the $p75^{NTR}$ extracellular domain have been described (Delbary-Gossart et al., 2016; Massa et al., 2006). In the absence of structural information, it is uncertain whether these molecules engage $p75^{NTR}$ directly and, if so, which is the nature of their molecular mechanisms of action. It is also unclear whether they function as agonists or antagonists with regard to the different pathways activated by this receptor. Due to the large molecular surfaces through which they engage ligands and effectors, growth factor receptors, particularly non-catalytic receptors such as $p75^{NTR}$, are difficult to target with small molecules. On the other hand, TMDs are small and critically involved in conformational coupling across the plasma membrane. TMD interfaces in receptor complexes are highly dynamic (Arkhipov et al., 2013) and form pockets that are amenable to binding by small molecules. Admittedly, compounds targeting receptor TMDs are likely to display moderate-to-high hydrophobicity. However, different delivery strategies, including various encapsulations, liposome formulations, and spray-dried nanocrystals, have been developed in

recent years that are expected to greatly facilitate their application (Hou et al., 2017; Schwendener and Schott, 2010; Wischke and Schwendeman, 2008). Interestingly, although the thrombopoietin mimic SB394725 was initially identified on the basis of its activity (Erickson-Miller et al., 2005), it was later found to target the TMD of the thrombopoietin receptor (Kim et al., 2007). To our knowledge, NSC49652 is the first compound identified in a screen specifically designed to affect growth factor receptor TMDs.

Melanoma is the most serious form of skin cancer and among the most common cancers in the United States, causing 87,000 cases and 9,700 deaths annually (Siegel et al., 2017). Worldwide, melanoma accounts for 352,000 cases and 60,000 deaths annually (Fitzmaurice et al., 2015). Melanoma is highly metastatic to brain and lung, and patients with invasive melanoma have a very high mortality rate. Selective inhibitors of BRAF, such as vemurafenib and dabrafenib, have induced tumor regression and prolonged overall survival in patients with metastatic melanoma containing mutated forms of BRAF, which have been estimated to be present in 40%–50% of all melanoma patients (Davies et al., 2002). However, virtually every patient treated with BRAF inhibitor eventually develops resistance and has disease progression (Chapman et al., 2011). No consistent mechanism of resistance has been identified. The other protein that can be effectively targeted in patients with melanoma is mutant KIT, but activating mutations of KIT have been found in only a small percentage of all melanoma cases. Thus, over 50% of melanoma cancers lack a clear target for therapeutic intervention, and, in those that do, resistance is an ensuing problem. $p75^{NTR}$ is present at high levels in different types of melanomas and is a marker of melanoma tumor-initiating cells (Boiko et al., 2010), therefore targeting $p75^{NTR}$ may potentially benefit multiple classes of melanoma tumors. In our studies, tumor growth of A875 cells expressing $p75^{NTR}$ was significantly reduced, and survival improved in mice treated with NSC49652. Increased cell death in the tumors from animals treated with NSC49652 suggests that the compound limited tumor growth through cytotoxic effects on tumor cells. The fact that it did not affect tumor cells lacking $p75^{NTR}$ suggests that these effects were mediated through the intended target. Interestingly, $p75^{NTR}$ has also been implicated in melanoma cell migration (Shonukan et al., 2003), warranting further studies on the possible effects of NSC49652 or related compounds on metastasis models of melanoma.

More generally, our results show that TMDs represent attractive targets for small-molecule manipulation of receptor function. Many other growth factor receptors form pre-formed complexes in which their TMDs play important roles, including receptor tyrosine kinases and transforming growth factor β superfamily receptors (Shen and Maruyama, 2012; Zhu and Sizeland, 1999). Our studies suggest that several classes of different receptors could be targeted with this approach.

SIGNIFICANCE

Small molecules offer a powerful way to alter protein function to produce dose-dependent agonistic or antagonistic effects that are acute and reversible in cells and organisms. Chemical probes that selectively modulate protein function can also serve as leads for the development of novel therapeutics. Most proteins in the human proteome, however, lack chemical probes. Several protein classes are even perceived to be potentially "undruggable," i.e., unsuitable for chemical probe development. Among these, are the large class of non-catalytic transmembrane receptors, including death receptors of the tumor necrosis factor receptor (TNFR) superfamily. This class of proteins lack intrinsic enzymatic activity and normally function by binding to other proteins, both extracellular and intracellular, through relatively large molecular surfaces, making it difficult for small molecules to interfere with such interactions. Ligand binding to transmembrane receptors induces conformational changes that are transmitted through the transmembrane domains (TMDs) to affect the intracellular domain. TMDs are therefore critical structural elements for information transfer across the plasma membrane in these receptors. The question then arises whether TMDs are suitable targets for small molecules to affect receptor function. We hypothesized that small molecules targeting the interfaces between TMDs in receptor complexes may induce conformational changes that alter receptor function. Applying this concept in a screening assay, we identified a compound targeting the TMD of death receptor $p75^{NTR}$, which induced profound conformational changes and receptor activity. The compound triggered apoptotic cell death dependent on $p75^{NTR}$ and JNK activity in neurons and melanoma cells, and inhibited tumor growth in a melanoma mouse model. More generally, our results show that TMDs represent attractive targets for small-molecule manipulation of receptor function. Many growth factor receptors form pre-formed complexes involving their TMDs. Our studies suggest that several classes of different receptors could be targeted with this approach.

STAR★METHODS

Detailed methods are provided in the online version of this paper and include the following:

- KEY RESOURCES TABLE
- CONTACT FOR REAGENT AND RESOURCE SHARING
- EXPERIMENTAL MODEL AND SUBJECT DETAILS
- METHOD DETAILS
  - Chemicals and Antibodies
  - AraTM Screening Assay
  - NMR Sample Preparation, Spectroscopy and Structure Calculations
  - Homo-FRET Anisotropy Microscopy
  - Cell Culture and Immunoblotting
  - Cell Viability, Cell Growth Rate and Cell Cycle Analyses
  - Pharmacokinetics and Toxicology
  - Melanoma Tumor Growth Assay
  - TUNEL Assay
- QUANTIFICATION AND STATISTICAL ANALYSIS
- DATA AND SOFTWARE AVAILABILITY
  - Data Availability
  - Software Availability

SUPPLEMENTAL INFORMATION

Supplemental Information includes five figures and can be found with this article online at https://doi.org/10.1016/j.chembiol.2018.09.007.

ACKNOWLEDGMENTS

We thank Liam Good (The Royal Veterinary College, London, UK) for the AS19 bacterial strain, Jason Tann, Lilian Kisiswa, and Daniel Su for help with preliminary studies, and Goh Ket Yin for technical assistance. Support for this research was provided by grants to C.F.I. from the Swedish Research Council, Swedish Cancer Society, Knut and Alice Wallenbergs Foundation (Wallenberg Scholars Program), and the National University of Singapore, and to D.L.S. from the Canadian Cancer Society and Robert C. Westbury Endowment.

AUTHOR CONTRIBUTIONS

E.T.H.G. developed the screening assay, conducted the primary screen, and performed validation experiments shown in Figures 3B–3D, 4A–4G, and S1. Z.L. performed all NMR studies. B.Y.A. and N.H.D. perform all *in vivo* cancer studies and the *in vitro* studies shown in Figures 4I and S4D. V.L.-R. performed the experiments shown in Figures 2D, 2E, 3D, 4H, S2A–S2D, and S4A–S4C. S.S. performed the experiments shown in Figures 1C and S2E. B.B. provided materials and advice for the AraTM assay. B.D. provided assistance with medicinal chemistry and curated the collection of NSC49652 analogs shown in Figure S1B. D.L.S. designed and supervised all cancer studies. C.F.I. conceived the original hypothesis and strategy, participated in experimental design, coordinated the work, and wrote the manuscript.

DECLARATION OF INTERESTS

The authors declare no competing interests.

Received: April 16, 2018
Revised: June 24, 2018
Accepted: September 11, 2018
Published: October 4, 2018

REFERENCES

Arkhipov, A., Shan, Y., Das, R., Endres, N.F., Eastwood, M.P., Wemmer, D.E., Kuriyan, J., and Shaw, D.E. (2013). Architecture and membrane interactions of the EGF receptor. Cell *152*, 557–569.

Boiko, A.D., Razorenova, O.V., van de Rijn, M., Swetter, S.M., Johnson, D.L., Ly, D.P., Butler, P.D., Yang, G.P., Joshua, B., Kaplan, M.J., et al. (2010). Human melanoma-initiating cells express neural crest nerve growth factor receptor CD271. Nature *466*, 133–137.

Case, D.A., Cheatham, T.E., Darden, T., Gohlke, H., Luo, R., Merz, K.M., Onufriev, A., Simmerling, C., Wang, B., and Woods, R.J. (2005). The Amber biomolecular simulation programs. J. Comput. Chem. *26*, 1668–1688.

Chapman, P.B., Hauschild, A., Robert, C., Haanen, J.B., Ascierto, P., Larkin, J., Dummer, R., Garbe, C., Testori, A., Maio, M., et al. (2011). Improved survival with vemurafenib in melanoma with BRAF V600E mutation. N. Engl. J. Med. *364*, 2507–2516.

Davies, H., Bignell, G.R., Cox, C., Stephens, P., Edkins, S., Clegg, S., Teague, J., Woffendin, H., Garnett, M.J., Bottomley, W., et al. (2002). Mutations of the BRAF gene in human cancer. Nature *417*, 949–954.

Delaglio, F., Grzesiek, S., Vuister, G.W., Zhu, G., Pfeifer, J., and Bax, A. (1995). NMRPipe: a multidimensional spectral processing system based on UNIX pipes. J. Biomol. NMR *6*, 277–293.

Delbary-Gossart, S., Lee, S., Baroni, M., Lamarche, I., Arnone, M., Canolle, B., Lin, A., Sacramento, J., Salegio, E.A., Castel, M.-N., et al. (2016). A novel inhibitor of p75-neurotrophin receptor improves functional outcomes in two models of traumatic brain injury. Brain *139*, 1762–1782.

Endres, N.F., Das, R., Smith, A.W., Arkhipov, A., Kovacs, E., Huang, Y., Pelton, J.G., Shan, Y., Shaw, D.E., Wemmer, D.E., et al. (2013). Conformational coupling across the plasma membrane in activation of the EGF receptor. Cell *152*, 543–556.

Erickson-Miller, C.L., Delorme, E., Tian, S.-S., Hopson, C.B., Stark, K., Giampa, L., Valoret, E.I., Duffy, K.J., Luengo, J.I., Rosen, J., et al. (2005). Discovery and characterization of a selective, nonpeptidyl thrombopoietin receptor agonist. Exp. Hematol. *33*, 85–93.

Ferrao, R., and Wu, H. (2012). Helical assembly in the death domain (DD) superfamily. Curr. Opin. Struct. Biol. *22*, 241–247.

Fitzmaurice, C., Dicker, D., Pain, A., Hamavid, H., Moradi-Lakeh, M., MacIntyre, M.F., Allen, C., Hansen, G., Woodbrook, R., Wolfe, C., et al. (2015). The global burden of cancer 2013. JAMA Oncol. *1*, 505–527.

Good, L., Sandberg, R., Larsson, O., Nielsen, P.E., and Wahlestedt, C. (2000). Antisense PNA effects in *Escherichia coli* are limited by the outer-membrane LPS layer. Microbiology *146* (Pt 10), 2665–2670.

Grigoryan, G., Moore, D.T., and DeGrado, W.F. (2011). Transmembrane communication: general principles and lessons from the structure and function of the M2 proton channel, K^+ channels, and integrin receptors. Annu. Rev. Biochem. *80*, 211–237.

Herrmann, T., Güntert, P., and Wüthrich, K. (2002). Protein NMR structure determination with automated NOE assignment using the new software CANDID and the torsion angle dynamics algorithm DYANA. J. Mol. Biol. *319*, 209–227.

Hou, Y., Shao, J., Fu, Q., Li, J., Sun, J., and He, Z. (2017). Spray-dried nanocrystals for a highly hydrophobic drug: increased drug loading, enhanced redispersity, and improved oral bioavailability. Int. J. Pharm. *516*, 372–379.

Ichim, G., Tauszig-Delamasure, S., and Mehlen, P. (2012). Neurotrophins and cell death. Exp. Cell Res. *318*, 1221–1228.

Johnson, B.A., and Blevins, R.A. (1994). NMR View: a computer program for the visualization and analysis of NMR data. J. Biomol. NMR *4*, 603–614.

Kim, M.-J., Park, S.H., Opella, S.J., Marsilje, T.H., Michellys, P.-Y., Seidel, H.M., and Tian, S.-S. (2007). NMR structural studies of interactions of a small, nonpeptidyl Tpo mimic with the thrombopoietin receptor extracellular juxtamembrane and transmembrane domains. J. Biol. Chem. *282*, 14253–14261.

Koradi, R., Billeter, M., and Wüthrich, K. (1996). MOLMOL: a program for display and analysis of macromolecular structures. J. Mol. Graph. *14*, 51–55, 29–32.

Laskowski, R.A., Rullmannn, J.A., MacArthur, M.W., Kaptein, R., and Thornton, J.M. (1996). AQUA and PROCHECK-NMR: programs for checking the quality of protein structures solved by NMR. J. Biomol. NMR *8*, 477–486.

Lee, K.F., Li, E., Huber, L.J., Landis, S.C., Sharpe, A., Chao, M.V., and Jaenisch, R. (1992). Targeted mutation of the gene encoding the low affinity NGF receptor P75 leads to deficits in the peripheral sensory nervous-system. Cell *69*, 737–749.

Lin, Z., Sriskanthadevan, S., Huang, H., Siu, C.-H., and Yang, D. (2006). Solution structures of the adhesion molecule DdCAD-1 reveal new insights into Ca(2+)-dependent cell-cell adhesion. Nat. Struct. Biol. *13*, 1016–1022.

Lin, Z., Tann, J.Y., Goh, E.T.H., Kelly, C., Lim, K.B., Gao, J.F., and Ibáñez, C.F. (2015). Structural basis of death domain signaling in the p75 neurotrophin receptor. Elife *4*, e11692.

Massa, S.M., Xie, Y., Yang, T., Harrington, A.W., Kim, M.L., Yoon, S.O., Kraemer, R., Moore, L.A., Hempstead, B.L., and Longo, F.M. (2006). Small, nonpeptide p75NTR ligands induce survival signaling and inhibit proNGF-induced death. J. Neurosci. *26*, 5288–5300.

Nadezhdin, K.D., García-Carpio, I., Goncharuk, S.A., Mineev, K.S., Arseniev, A.S., and Vilar, M. (2016). Structural basis of p75 transmembrane domain dimerization. J. Biol. Chem. *291*, 12346–12357.

Park, H.H., Logette, E., Raunser, S., Cuenin, S., Walz, T., Tschopp, J., and Wu, H. (2007). Death domain assembly mechanism revealed by crystal structure of the oligomeric PIDDosome core complex. Cell *128*, 533–546.

Pettersen, E.F., Goddard, T.D., Huang, C.C., Couch, G.S., Greenblatt, D.M., Meng, E.C., and Ferrin, T.E. (2004). UCSF Chimera – a visualization system for exploratory research and analysis. J. Comput. Chem. *25*, 1605–1612.

Russ, W.P., and Engelman, D.M. (1999). TOXCAT: a measure of transmembrane helix association in a biological membrane. Proc. Natl. Acad. Sci. USA *96*, 863–868.

Schwendener, R.A., and Schott, H. (2010). Liposome formulations of hydrophobic drugs. In Liposomes, V. Weissig, ed. (Humana Press), pp. 129–138.

Shen, J., and Maruyama, I.N. (2012). Brain-derived neurotrophic factor receptor TrkB exists as a preformed dimer in living cells. J. Mol. Signal. *7*, 2.

Shonukan, O., Bagayogo, I., McCrea, P., Chao, M.V., and Hempstead, B.L. (2003). Neurotrophin-induced melanoma cell migration is mediated through the actin-bundling protein fascin. Oncogene *22*, 3616–3623.

Siegel, R.L., Miller, K.D., and Jemal, A. (2017). Cancer Statistics, 2017. CA Cancer J. Clin. *67*, 7–30.

Su, P.-C., and Berger, B.W. (2012). Identifying key juxtamembrane interactions in cell membranes using AraC-based transcriptional reporter assay (AraTM). J. Biol. Chem. *287*, 31515–31526.

Su, P.-C., and Berger, B.W. (2013). A novel assay for assessing juxtamembrane and transmembrane domain interactions important for receptor heterodimerization. J. Mol. Biol. *425*, 4652–4658.

Sykes, A.M., Palstra, N., Abankwa, D., Hill, J.M., Skeldal, S., Matusica, D., Venkatraman, P., Hancock, J.F., and Coulson, E.J. (2012). The effects of transmembrane sequence and dimerization on cleavage of the p75 neurotrophin receptor by γ-secretase. J. Biol. Chem. *287*, 43810–43824.

Tanaka, K., Kelly, C.E., Goh, K.Y., Lim, K.B., and Ibáñez, C.F. (2016). Death domain signaling by disulfide-linked dimers of the p75 neurotrophin receptor mediates neuronal death in the CNS. J. Neurosci. *36*, 5587–5595.

Underwood, C.K., and Coulson, E.J. (2008). The p75 neurotrophin receptor. Int. J. Biochem. Cell Biol. *40*, 1664–1668.

Vicario, A., Kisiswa, L., Tann, J.Y., Kelly, C.E., and Ibáñez, C.F. (2015). Neuron-type-specific signaling by the p75NTR death receptor is regulated by differential proteolytic cleavage. J. Cell Sci. *128*, 1507–1517.

Vilar, M., Charalampopoulos, I., Kenchappa, R.S., Simi, A., Karaca, E., Reversi, A., Choi, S., Bothwell, M., Mingarro, I., Friedman, W.J., et al. (2009). Activation of the p75 neurotrophin receptor through conformational rearrangement of disulphide-linked receptor dimers. Neuron *62*, 72–83.

Wischke, C., and Schwendeman, S.P. (2008). Principles of encapsulating hydrophobic drugs in PLA/PLGA microparticles. Int. J. Pharm. *364*, 298–327.

Zhu, H.J., and Sizeland, A.M. (1999). A pivotal role for the transmembrane domain in transforming growth factor-beta receptor activation. J. Biol. Chem. *274*, 11773–11781.

STAR★METHODS

KEY RESOURCES TABLE

REAGENT or RESOURCE	SOURCE	IDENTIFIER
Antibodies		
$p75^{NTR}$ extracellular domain	Alomone	ANT-007
Actin	Cell Signaling Technol.	4967
Cleaved caspase-3	Cell Signaling Technol.	9664
PARP	Cell Signaling Technol.	9542
GAPDH	Sigma Aldrich	G9545
Rabbit IgG HRP	Thermo Fisher	31460
Mouse anti-BrdU	BD Bioscience	347580
Bacterial and Virus Strains		
Escherichia coli AS19	Dr. Liam Good (RVC, UK)	
Escherichia coli SoluBL21 (DE3)	Genlantis, USA	C700200
Chemicals, Peptides, and Recombinant Proteins		
Dodecyl phosphocholine-d38	Avanti, USA	860336
n-dodecylphosphocholine	Avanti, USA	850336
n-nonyl-ß-D-glucoside	Avanti, USA	850510
DEUTERIUM OXIDE (D, 99.96%)	Cambridge Isotope Labs	DLM-6-10X0.7
AMMONIUM CHLORIDE (15N, 99%),	Cambridge Isotope Labs	NLM-467-50
D-GLUCOSE (U-13C6, 99%)	Cambridge Isotope Labs	CLM-1396-50
DIMETHYL SULFOXIDE-D6 "100%" (D, 99.96%)	Cambridge Isotope Labs	DLM-34
Ni-NTA Agarose	Qiagen	30230
Superdex 200 Increase 10/300 GL	GE	28990944
Collagen I rat protein, tail	Gibco	A1048301
Fugene HD transfection reagent	Promega	E2311
Spectinomycin	Gold Biotechnology	S-140-25
Geneticin Selective Antibiotic	Gibco	10131035
Amphicilin	Gold Biotechnology	A-301-100
IPTG	Gold Biotechnology	I2481C50
Anisomycin	Tocris	1290
NSC49652	Glixx Laboratories and SAI Life India	Custom order
Dulbecco's phosphate buffered saline (DPBS)	Invitrogen	14190
Eco-mount	Biocare Medical	EM897L
EDTA	Invitrogen	15576-028
Fetal bovine serum	Invitrogen	12483-020
FuGene 6	Promega	E2691
G418	Invitrogen	10131035
Glucose	Sigma-Aldrich	G7528
Hematoxylin solution, Gill No-2	Sigma-Aldrich	GHS232
L-glutamine	Invitrogen	25030-081
Liquid DAB+ substrate chromogen system	Dako	K3468
Propidium iodide (PI)	Sigma-Aldrich	P4170
Puromycin	Calbiochem	540411
RNase A	Sigma-Aldrich	R6513
Rodent Block M	Biocare Medical	RBM9611
Rodent-Decloaker	Biocare Medical	RD913M
sodium carboxymethyl cellulose	Sigma-Aldrich	21902

(*Continued on next page*)

Continued

REAGENT or RESOURCE	SOURCE	IDENTIFIER
Sodium pyruvate	Invitrogen	11360-070
Triton X-100	Sigma-Aldrich	T9284
Critical Commercial Assays		
Alamar Blue	Invitrogen	Dal1100
Q5 Site directed mutagenesis	New England Biolabs	E0554S
Envision and System-HRP Kit	DAKO	K4007
In situ cell death detection kit (TUNEL), fluorescein	Sigma-Aldrich (Roche)	11684795910
Experimental Models: Cell Lines		
Green monkey: COS-7	ATCC	CRL-1651
Human: A875 melanoma	ATCC	n.a.
Human: A875 GFPLuc NT	This paper	n.a.
Human: A875 GFPLuc shp75	This paper	n.a.
Experimental Models: Organisms/Strains		
CB17 SCID mice (8-week-old female)	Charles River Laboratory	Strain code 236
Oligonucleotides		
shp75 oligo sense; 5'GATCCAATTGCCATTTACTACAGTGCCTCGA GGCACTGTAGTAAATGGCAATTTTTTTG3'	University of Calgary DNA core service	n.a.
shp75 oligo anti-sense; 5'AGCTTCAAAAAAATTGCCATTTACTACAGTG CCTCGAGGCACTGTAGTAAATGGCAATTG3'	University of Calgary DNA core service	n.a.
Non-targeting oligo sense; 5'GATCCCAACAAGATGAAGAGCACCAACTC GAGTTGGTGCTCTTCATCTTGTTGTTTTTG3'	University of Calgary DNA core service	n.a.
Non-targeting oligo anti-sense; 5'AGCTTCAAAAACAACAAGATGAAGAGCACC AACTCGAGTTGGTGCTCTTCATCTTGTTGG3'	University of Calgary DNA core service	n.a.
Recombinant DNA		
pM-p75TMD	This paper	n.a.
pcDNA3-rat p75-EGFP (A207K)	Ibanez lab	n.a.
PiggyBac shRNA vector	System Bioscience	PBSI505A-1
Software and Algorithms		
NMRPipe	National Institutes of Health	https://spin.niddk.nih.gov/bax/software/NMRPipe/NMRPipe.html
NMRView	One Moon Scientific, Inc	http://www.onemoonscientific.com/
DYANA/CYANA	University of Frankfurt	http://www.cyana.org
UCSF Chimera	University of California San Francisco	https://www.cgl.ucsf.edu/chimera/
PROCHECK-NMR	European Molecular Biology Laboratory	https://www.ebi.ac.uk/thornton-srv/software/PROCHECK/
Image J	NIH	https://imagej.nih.gov
MatLab	Mathworks	www.mathworks.com
CellQuest	BD Bioscience	n.a.
CellSense Standard	Olympus	n.a.
GraphPad Prism 6	Graphpad software	n.a.
In Cell developer toolbox 1.9.1	GE healthcare	n.a.
Living Image	Xenogen	n.a.
Modfit LT	Verity	n.a.
Volocity	Perkin Elmer	n.a.
Deposited Data		
Coordintates of $p75^{NTR}$ TMD	Nadezhdin et al. (2016)	PDB: 2MIC
Coordinates of $p75^{NTR}$ TMD:NSC49652 complex	This study	PDB: 5ZGG

CONTACT FOR REAGENT AND RESOURCE SHARING

For reagents and resources generated in this study, other than A875-GFPLuc NT or shp75 cells, or any other questions about the reagents please contact Carlos F. Ibáñez (phscfi@nus.edu.sg). For all questions and inquiries regarding A875-GFPLuc NT or shp75 cells please contact Donna L. Senger (senger@ucalgary.ca).

EXPERIMENTAL MODEL AND SUBJECT DETAILS

This study uses the following cell lines: COS7 green monkey kidney fibroblasts; and human melanoma cells A875, 70W and 3S5. The sex of these cell lines is unknown. COS7 and melanoma cells A875, 70W and 3S5 were cultured under standard conditions in DMEM supplemented with 10% fetal calf serum, 100 units/ml penicillin, 100 mg/ml streptomycin, and 2.5 mM glutamine. Culture condition for CGNs were as described in (Vicario et al., 2015). Primary cultures of cerebellar granule neurons were derived from C57/Bl6 mouse or Sprague-Dawley rat pups of both sexes. Severe combined immunodeficient (SCID) mice used in the melanoma tumor growth assay were all females. SCID mice are immunodeficient and homozygous for the severe combined immune deficiency spontaneous mutation *Prkdc*^{scid} and ; C57/Bl6 mice have a *wild type* genotype; Sprague-Dawley rats have a *wild type* genotype. p75^{NTR} knock-out mice are homozygous for a null mutation in the *Ngfr* locus. p75^{NTR} delta-DD and C259A mice are knock-in mice carrying either a deletion of exons 5 and 6 or a substitution at amino acid position 259, respectively, in the mouse *Ngfr* locus. Husbandry and housing conditions of experimental animals were in accordance with Swedish and Canadian law regulations and approved by the corresponding insttution ethical committees.

METHOD DETAILS

Chemicals and Antibodies

Diversity V library was obtained from National Cancer Institute (Division of Cancer Treatment and Diagnosis, Developmental Therapeutics Program, http://dtp.cancer.gov). NSC49652 was custom synthesized by Glixx Laboratories and SAI Life India at a purity greater than 98%. NGF was purchased from R&D Systems. JNK-IN-8 was obtained from the Division of Signal Transduction Therapy, Dundee University. Antibodies against p75^{NTR} extracellular domain were obtained from Alomone Labs (ANT-007). Antibodies against α-actin, cleaved Caspase 3, and PARP were from Cell Signaling Technologies. Antibodies against BrdU were from BD Biosciences.

AraTM Screening Assay

The screening assay was based on the AraTM assay to assess conformation changes and binding strength in a pair of interacting TMDs (Su and Berger, 2012; 2013). cDNA corresponding to the human p75^{NTR} TMD (NLIPVYCSILAAVVVGLVAYIAFKRW) was subcloned in the KpnI and SacI restriction sites of the AraTM chimera plasmid. *E. coli* strain AS19 lacks LPS, allowing the uptake of a variety of molecules, peptides and nuclei acids (Good et al., 2000). A single colony of AS19 transformants carrying the p75^{NTR} TMD–AraTM chimera and GFP reporter plasmids were grown overnight in LB medium supplemented with 50 μg/ml spectinomycin and 100 μg/ml ampicillin. The culture was then diluted 1:100 in fresh LB medium and allowed to grow till optical density (OD) 630 reached between 0.2 and 0.5 after which IPTG was added to a final concentration of 1mM to induce the expression of the p75^{NTR} TMD–AraTM chimera. 100 μl of this culture were dispensed into black-rim clear bottom 96-well plates (Corning #3631) that had been preloaded with 0.5 μl of 10 mM solution of stock compounds in triplicate (50μM final concentration). The plates were incubated with vigorous shaking at 38°C for 4 hs to allow IPTG-induced expression of the p75^{NTR} TMD–AraTM chimeric protein. The plates were then centrifuged at 4000 rpm for 10 min at room temperature to pellet bacteria. LB media was aspirated and replaced with 100 μl of Phosphate Buffered Saline (PBS), and bacteria cells were resuspended by vigorous shaking for 10 min. GFP signal was measured in each well (excitation 475nm, emission 509 nm) and bacterial density was determined by measurement of OD_{630} in a microplate plate reader (BioTek).

NMR Sample Preparation, Spectroscopy and Structure Calculations

Human p75^{NTR} cDNA encoding residues 244 to 277, encompassing the p75^{NTR} TMD, and N-terminally tagged with a 6xHis epitope was subcloned in the pET32 expression vector. SoluBL21 (DE3) bacterial cells carrying this plasmid were grown in M9 minimal medium containing ^{15}N-NH_4Cl and ^{13}C-labeled glucose as the sole source of nitrogen and carbon. Cells were lysed by sonication. Unbroken cells were removed by centrifugation at 6,000 g for 30 min. The membrane fraction was collect by 100,000 g centrifugation at 4°C for 30 min. The p75^{NTR} TMD was extracted from the membrane fraction with Octyl β-D-glucopyranoside and purified by Ni-NTA affinity chromatography and FPLC gel filtration. Protein:drug complexes were prepared by mixing 0.8 mM ^{13}C,^{15}N-labeled p75^{NTR} TMD and 3.9 mM NSC49652 in 200 mM deuterated dodecylphosphocholine-d38 (DPC-d38), 5% deuterated dimethyl sulfoxide-d6 (DMSO-d6), 5 mM phosphate buffer at pH 6.0. The dimerization of p75^{NTR} TMD was confirmed by non-reducing 12 % Tricine SDS PAGE (Figure S3A).

NMR experiments were performed on a Bruker 800 MHz NMR spectrometer with a cryogenic probe at 40°C. All spectra were processed with NMRPipe (Delaglio et al., 1995) and analyzed with NMRView supported by a NOE assignment plugin (Johnson and Blevins, 1994). Resonance assignments of backbone and aliphatic side chains of p75^{NTR} TMS were obtained using [^1H-^{15}N] HSQC, [^1H-^{13}C] HSQC, 3D HNCA, 3D HN(CO)CA, 3D HCCH-TOCSY, and 3D ^{13}C, ^{15}N-edited NOESY spectra. Aromatic side chains assignments of p75^{NTR} TMD were obtained using previously described methods (Lin et al., 2006). 1HCC resonances of NSC49652

were assigned using 2D ^{13}C,^{15}N-filtered TOCSY spectrum. Intramolecular NOE restraints were obtained from 3D ^{13}C, ^{15}N-edited NOESY spectra. Protein:drug NOEs were identified from 2D and 3D ^{13}C,^{15}N-filtered NOESY spectra. Ambiguous NOEs were assigned with iterated structure calculations by DYANA (Herrmann et al., 2002). Final structure calculation was started from 100 conformers. Energy minimization of the 10 conformers with the lowest final target function values was performed in AMBER force field (Case et al., 2005). The mean structure was obtained from the 10 energy-minimized conformers. PROCHECK-NMR (Laskowski et al., 1996) was used to assess the quality of the structures. All the structural figures were made using MOLMOL (Koradi et al., 1996) or Chimera (Pettersen et al., 2004). The coordinates of the $p75^{NTR}$ TMD: NSC49652 complex are available in the Protein Data Bank (PDB ID 5ZGG).

Homo-FRET Anisotropy Microscopy

Anisotropy microscopy was done as previously described (Lin et al., 2015; Tanaka et al., 2016) in COS-7 cells that were transiently transfected with a rat $p75^{NTR}$-EGFP* fusion construct as previously described (Vilar et al., 2009). EGFP* denotes a monomeric A207K EGFP mutant. Wild type, Cys^{257}Ala and Pro^{254}Gly mutants (rat $p75^{NTR}$ numbering) were used in these experiments, as indicated. We note that the TMDs of human and rat $p75^{NTR}$ are identical in sequence. Changes in anisotropy were expressed as fold change at each time point in comparison to the mean of 6 time points obtained prior to addition of vehicle or NSC49652 (20μM).

Cell Culture and Immunoblotting

COS7 and melanoma cells A875, 70W and 3S5 were cultured under standard conditions in DMEM supplemented with 10% fetal calf serum, 100 units/ml penicillin, 100 mg/ml streptomycin, and 2.5 mM glutamine. For live cell FRET anisotropy studies, COS cells were transfected using FuGENE 6 as previously described (Tanaka et al., 2016). Cultures of rat CGNs were made essentially as previously described (Vicario et al., 2015) using cerebella from postnatal day 5 (P5) rat pups or P7 mouse pups as indicated. The generation of $p75^{NTR}$ mutant mice knock-out (exon 3), delta-DD, and C259A have been described previously (Lee et al., 1992; Tanaka et al., 2016). All mice were backcrossed to a C57/Bl6 background. CGNs were plated at $1x10^6$ cells per cm^2 on 6-well culture plates pre-coated 0.01% (W/V) poly-D-Lysine (Sigma). Cells were allowed to settle for 48h prior to experiments. A875-GFPLuc cells (i.e. A875 constitutively expressing GFP and luciferase) were grown under standard conditions in DMEM supplemented with 10% fetal calf serum, 2.5 mM glutamine and 400 μg/ml G418. A875-GFPLuc cells deficient in $p75^{NTR}$ expression were generated by shRNA knock-down. Briefly, $p75^{NTR}$ shRNA (target sequence: GCACTGTAGTAAATGGCAATT) was synthesized, annealed and inserted into the BamHI and EcoRI sites of PiggyBac shRNA vector (PBSI505A-1, System Bioscience). The PiggyBac non-targeting (NT) vector contains a shRNA insert (sequence; CAACAAGATGAAGAGCACCAA, sequence from System Bioscience) that does not target any known genes from any species. The sequences of the mutant expression plasmids were confirmed prior to stable transfection. A875-GFPLuc cells were transfected using FuGENE 6, (Roche, Indianapolis, IN) according to the manufacturer's instructions. The following day, the culture media was changed to fresh complete media containing puromycin (2 μg/ml) to select for cells expressing the shRNA. Cells were grown under antibiotic selection until confluent. Flow cytometry and Western blotting confirmed transfection and efficient knock-down of endogenous $p75^{NTR}$ expression (Figure S4A). Stable transfectants of $p75^{NTR}$ knock-down (shp75) or non-targeting (NT) A875-GFPLuc cells were cultured in identical media supplemented with both 400 μg/ml G418 and 2 μg/ml puromycin and passaged for 1 to 2 weeks. After that, the cells were maintained in identical media without puromycin. A875-GFPLuc cells were passaged by harvesting with Puck's EDTA solution (4 mM, NaHCO3; 136 mM, NaCl; 4 mM, KCl; 1 mM, EDTA; 1 mg/ml, glucose) at 80-90% confluence. To make sure to have a pure strain, both antibiotics were added every once in a month. For analysis of apoptosis, NGF (100ng/ml) or NSC49652 were added during 4 hs before cell lysis. Cell lysis and whole cell protein extraction were carried out in lysis buffer containing 50 mM Tris/HCl pH 7.5, 1 mM EDTA, 270 mM Sucrose, 1% (v/v) Triton X-100, 1 mM benzamidine, 1 mM PMSF, 0.1% (v/v) 2-mercaptoethanol and phosSTOP phosphatase inhibitor cocktail mix (Roche). Protein concentration was determined by the Bradford assay. Following SDS-PAGE and Western blotting, the immunoblots were developed using the ECL Western Blotting Kit (Thermo Scientific) and exposed to Kodak X-Omat AR films.

Cell Viability, Cell Growth Rate and Cell Cycle Analyses

To measure the cytotoxic effect of NSC49652, A875-GFPLuc NT or shp75 cells were seeded at 2,000 cells per well (in 100 μL DMEM) in a 96-well plate and incubated for 12h. Next, NSC49652 in 0.05% (v/v) DMSO at various concentrations was added and incubated at 37°C in 5% CO2 for 3 days. Following treatment, 10μL AlamarBlue® (resazurin, ThermoFIsher) was added to each well of the 96-well plate and incubated for 4 hours at 37°C in 5% CO2. Cellular fluorescence in each well was measured at 570 nm using a microtiter plate reader. Data was converted into the relative cell viability (%) from the absorbance of cells in each treatment relative to that of the DMSO control group (set as 100%). For cell rate growth, $1.5x10^5$ A875-GFPLuc control (NT) and knock-down (shp75) cells were plated and the number of viable cells was determined every 24hs during 4 consecutive days by trypan blue exclusion. To determine phase distribution of DNA content in A875 GFPLuc cells, PI (Propidium iodide) staining was performed followed by FACS flow cytometry. At least 10000 events were analyzed for each test sample. Data analyses were performed with Cell-Quest and Modfit software (Becton-Dickinson). The Student's t-test was used to compare data between cell lines.

Pharmacokinetics and Toxicology

Plasma pharmacokinetics of NCS49652 was investigated following single intravenous (3 mg/kg) or oral (10 mg/kg) dose administrations in C57BL/6 mice of both sexes. Blood samples were collected from the retro orbital plexus at pre-dose, 0.08, 0.25, 0.5, 1, 2, 5,

10 and 24 hs (for intravenous) and pre-dose, 0.25, 0.5, 1, 2, 4, 5, 10 and 24 hs (for oral). Toxicity of NCS49652 was tested in a 3 week repeated dose study in C57BL/6 mice following oral gavage administration. Pharmacokinetics and toxicology studies were carried out by Sai Life Sciences Limited, Hyderabad, India.

Melanoma Tumor Growth Assay

Eight-week-old female SCID mice (Charles River Laboratories, Shrewsbury, MA, USA) were housed in groups of three to five and maintained on a 12-h light/dark schedule with a temperature of 22 °C±1 °C and a relative humidity of 50%±5%. Food and water were available ad libitum. All procedures were reviewed and approved by the University of Calgary Animal Care Committee. A875-GFPLuc cells harvested using Puck's EDTA were resuspended in PBS and implanted subcutaneously into SCID mice ($1x10^6$ cells/200 μl per mouse). Animals were randomly divided into groups when tumor was confirmed by luciferase activity using a *in vivo* luciferase imaging system (Xenogen). NSC49652 was dissolved in 0.5% sodium carboxymethyl cellulose (CMC) and administered by oral gavage at 200 mg/kg/day during 3 weeks (i.e. 3 cycles, each consisting of 5 days on drug, 2 days off drug). The tumor size and body weight were measured using calipers every 2 days and luminescence was imaged once a week. The mice were sacrificed at an endpoint defined by the tumor volume (~2 cm). Tumor volume is calculated as volume = a x b x c (mm), a was the height, b was the shortest diameter, c was the longest diameter.

TUNEL Assay

Cell death in A875-GFPLuc tumor sections was detected by enzyme labeling of DNA strand breaks using a TUNEL assay (Roche, Switzerland) according to the manufacturer's instructions. Briefly, deparaffinized sections were incubated with a mixture of TdT and fluorescein–dUTP at 37°C for 1 hr to allow for labeling of free 3′-OH ends of genomic DNA. Following staining for TUNEL, sections were counterstained with DAPI for 5 min at 25°C and viewed using a fluorescent microscope. Quantification was obtained by counting the number of TUNEL positive cells in 3 independent fields of view (40X objective) from 2 mice treatment group. An apoptotic index was estimated by normalizing the number of TUNEL-positive cells to the total number of DAPI-positive cells in the field of view.

QUANTIFICATION AND STATISTICAL ANALYSIS

GraphPad Prism (version 4; GraphPad Software, Inc.) were used for statistical analyses, and survival curves were generated using the Kaplan–Meier method. Experimental data was collected from multiple experiments and reported as the treatment mean ± SEM. Significance was calculated using the Student t-test or one-way ANOVA where * indicates $p< 0.05$; **, $p< 0.01$ and ***, $p< 0.001$.

DATA AND SOFTWARE AVAILABILITY

Data Availability

Accession number: The NMR structure of p75NTR TMD in complex with NSC49652 has been deposited in the PDB database under ID code 5ZGG.

Software Availability

The software used for NMR studies was as follows: i) NMRPipe is a multidimensional spectral processing system based on UNIX pipes: https://spin.niddk.nih.gov/bax/software/NMRPipe/NMRPipe.html; ii) NMRView is a program for the visualization and analysis of NMR datasets: http://www.onemoonscientific.com/; iii) DYANA/CYANA is a program for NMR structural calculation: http://www.cyana.org; iv) PROCHECK-NMR is a program for checking the quality of structures solved by NMR: https://www.ebi.ac.uk/thornton-srv/software/PROCHECK/; v) UCSF Chimera is program for interactive visualization and analysis of molecular structures: https://www.cgl.ucsf.edu/chimera/. Other software is listed in the Key Resources Table.